



## The Impact of Effective Refractive Index on Fibre Bragg Grating Sensor Sensitivity for Structural Health Monitoring

<sup>1</sup>S. M. Sani, <sup>1</sup>A. D. Usman, <sup>1</sup>Obaje S. Peter, <sup>2</sup>Isyaku S. Falalu, <sup>1</sup>Agbon E. E.

<sup>1</sup>Department of Electronics and Telecommunications Engineering,  
Ahmadu Bello University, Zaria.

<sup>2</sup>Nigerian Television Authority, Kaduna.

### ABSTRACT

This research presents the impact of effective refractive index on Fibre Bragg Grating (FBG) sensor sensitivity for Structural Health Monitoring (SHM). SHM has been largely used in telecommunication, civil infrastructures, sports equipment, automotive, aerospace, oil and gas, and medical facilities due to their unique capability to monitor structures in a hazardous environment. In this research, the FBG sensitivity to induced strain on the composite structure was obtained at different effective refractive index values. The shifts in Bragg wavelength was plotted against the induced strain on the composite structure at effective refractive index values of  $n_{\text{eff}1} = 1$ ,  $n_{\text{eff}2} = 1.44$ ,  $n_{\text{eff}3} = 1.5$  and  $n_{\text{eff}4} = 2$  at Poisson's ratios ( $\nu$ ) of 0.3 and 0.19525. The simulation was carried out in MATLAB R2018a version which shows the FBG with the lowest effective refractive index result in the highest sensitivity. The result of the FBG with  $n_{\text{eff}2}$  was compared with that of  $n_{\text{eff}3}$ . The result shows that a 1.49% increment in sensitivity was obtained at Poisson's ratio ( $\nu$ ) of 0.3 and a 2.0% increment insensitivity was also achieved by the sensor when Poisson's ratio ( $\nu$ ) is 0.19525. The increment in the sensor's sensitivity enabled the FBG sensor to be suitable for monitoring structures in harsh environment.

### ARTICLE INFO

#### Article History

Received: December, 2020

Received in revised form: March, 2021

Accepted: April, 2021

Published online: May, 2021

### KEYWORDS

FBG, Effective refractive index, Bragg wavelength, Sensitivity, SHM, Strain.

### INTRODUCTION

Structural Health Monitoring (SHM) is a technology that aims at detecting, locating, and quantifying damage in structures at an early stage to prevent sudden failure [2]. Normally, deviations should be determined at an early stage of damage initiation and corrected by conducting suitable maintenance procedures, thereby improving structural integrity, reliability, availability and the overall life cycle of the structure [3]. This damage happens through a series of events such as extreme loading conditions and low-velocity impacts [15]. Which may compromise the integrity of the structure and raise safety issue [15]. Hence, the need to use SHM to detect damage at its early stage in composite materials is of high importance.

### LITERATURE REVIEW

[1] proposed a multiple ultrasonic waves-based Pause Array Monitoring for Enhanced Life Assessment (PAMELA) technique for structural health monitoring. The technique was intended to deliver various sorts of ultrasonic signals and direct them to the piezoelectric

transducers. Utilizing the PAMELA based configuration software, the ultrasonic waves to be transmitted to the hardware is chosen. Different damage detection values were obtained which described the advantages and peculiarities of metallic and composite materials.

[7] Proposed an efficient fast detection technique for multimode FBG sensor. The algorithm is based on a threshold detection window and a compensation centre of gravity for SHM. The Dynamic Gate Algorithm exhibited high vigour with a profoundly improved wavelength fit resolution compared with the traditional techniques and the computational speed was better than the Gaussian Fitting Algorithm for precise peak identification.

[10] Presented a distributed strain sensing using optical fibre sensing technology. Dynamic and distributed strains during the fatigue loading were quantified using the Brillouin Optical Correlation Domain Analysis (BOCDA) technique. The evaluated measurement of BOCDA, measured strain values were compared with that of FBG sensors. The dynamic strain measurement positions of BOCDA was

determined by the mean of measuring the length between the centre of the article and the FBG sensors using a tape measure. However, this work investigated the impact of the effective refractive index of FBG sensitivity to induced strain and how they can be quantified.

### FBG OPERATIONAL PRINCIPLE

FBG sensor is a periodic modulation of the refractive index of the core of an optical fibre as shown in Figure 1 [20]. The FBG reflects a specific wavelength that is, the Bragg wavelength which depends on the period of the grating ( $\Lambda$ ) and the effective refractive index ( $n_{eff}$ ) of the propagating mode back along with the optical fibre [11]. The uniform fibre Bragg grating sensor consists of an effective refractive index, a grating period and a Bragg wavelength respectively.

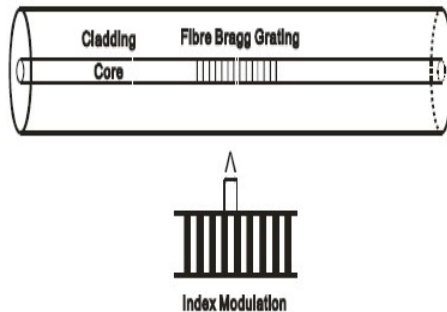


Figure 1: FBG Sensor (Chen & Ping, 2008).

### Photo Elastic Coefficient of FBG Sensor

Photo-elasticity describes the changes in the optical properties of an optical fibre material under mechanical deformation [6]. When mechanical strain is applied on the FBG sensor, the Bragg wavelength changes in both the effective refractive index and the periodicity of the grating [19]. The effective strain optic coefficient ( $p_e$ ) of an FBG sensor is obtained by the following: the effective refractive index ( $n_{eff}$ ), the Poisson's ratio ( $\nu$ ) and Pockel's coefficient ( $p_{11}$ ,  $p_{12}$ ) of the fibre optics sensor [5]. The change in the Bragg wavelength ( $\Delta\lambda_B$ ) is inversely proportional to the effective strain optics coefficient ( $p_e$ ) of the fibre optic sensor. In addition, Pockel's coefficient produces birefringence of the optical fibre sensor induced by an electric field and it is represented by  $p_{11}$  and  $p_{12}$  [18].

### FBG BASED SENSING MODEL

FBG sensing technology possesses a good multiplexing capability which enables it to

accommodate many grading and different sensing like; strain, temperature, water level, force, pressure, vibration, displacement, deformation just to mention a few in a single fibre optic cable [14]. FBG is a type of reflector etched in the core of an optical fibre that reflects particular wavelengths of light and transmits others, enabling its use as an optical sensor [12]. The centre of the fibre is surrounded by a silica cladding with a slightly lower index of refraction than the core which is between  $4\mu\text{m}$  and  $9\mu\text{m}$  diameter to enable the formation of a wavelength inside the fibre [12]. Each FBG is defined with a unique wavelength that changes with induced physical parameters. The refractive planes in the FBG are called Bragg planes, which are produced when two opposing light sources interfere constructively. Stretching a fibre Bragg grating causes a shift in the sensor's index of refraction [12] as shown below in Figure 2.

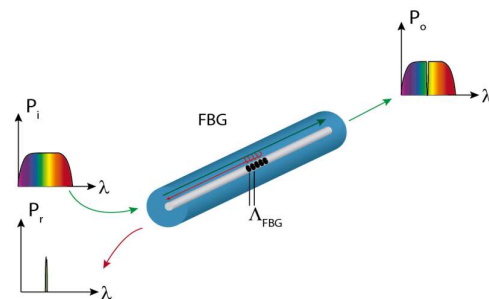


Figure 2: Fibre Bragg Grating Working Principle [8]

The grating wavelength is expressed in equation (1) [12]:

$$\lambda_B = 2n_{eff} \Lambda \quad (1)$$

where  $n_{eff}$  is the effective refractive index of the core mode at the Bragg wavelength,  $\Lambda$  is the grating period and  $\lambda_B$  is the Bragg wavelength. Equation (2) and (3) are the

expression for the FBG sensitivity and the effective strain optics coefficient as shown below:

$$\Delta\lambda_B = \lambda_B [1 - P_e] \quad (2)$$

$$P_e = \frac{n_{eff}^2}{2} \{p_{12} - \nu[(p_{11} + p_{12})]\} \quad (3)$$

where  $P_e$ ,  $\Delta\lambda_B$ ,  $\nu$ ,  $n_{eff}$ ,  $p_{11}$  and  $p_{12}$  are the effective strain optic coefficient, FBG sensitivity, Poisson's ratio, effective refractive index and Pockel's coefficient.

**Effective Refractive Index ( $n_{eff}$ ):**  $n_{eff}$  is a measure of the overall delay of the propagating light beam in the optical fibre (Harpreet, 2011).

Guided modes through the fibre core are defined by  $n_{eff}$  and  $v$ -parameter values (Rizwana *et al* 2018). The  $n_1$  is the core refractive index and  $n_2$  is the cladding refractive index modes propagation through waveguide must follow the condition specified by equation (4) and (5) (Rizwana *et al* 2018).

$$n_2 \leq n_{eff} \leq n_1 \quad (4)$$

$$n_{eff} = n_l + n_n \quad (5)$$

In equation (5) the first term denotes the linear refractive index and the second term is the refractive index variations due to non-linearities. The sum of both terms results in the effective refractive index of the FBG sensor as shown in equation (5) [16]. The flow chart of the proposed work is shown in Figure 3.

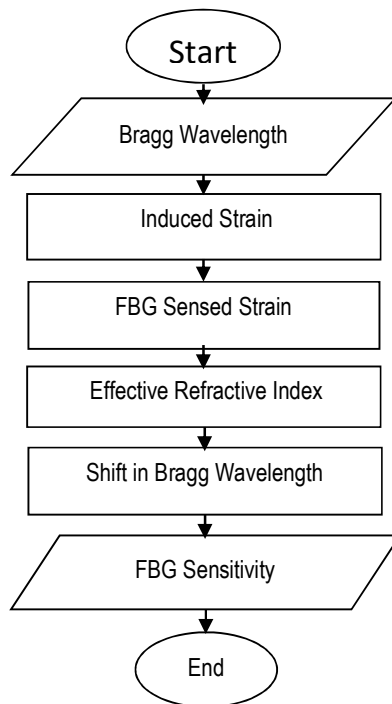


**Figure 3:** Flow Chart of the Impact of Effective Refractive Index on FBG Sensor Sensitivity

## RESULTS

The results obtained from the simulation result are discussed in this section. The following results are based on the shift in Bragg wavelength of the FBG due to induced strain at the different effective refractive difference.

In Figure 4, the shifts in Bragg wavelength was plotted against the induced strain on the composite structure at different effective refractive index values of the fibre ( $n_{eff1} = 1$ ,  $n_{eff2} = 1.44$ ,  $n_{eff3} = 1.5$  and  $n_{eff4} = 2$ ) when  $v$  is 0.3. The plot was obtained, from the simulation values in Table 1. Table 1 was generated using equations (2) and (3). From the plot, it is observed that the shift in Bragg wavelength is due to the different values of the effective refractive index ( $n_{eff}$ ) of the FBG sensor. From the plot, it is observed that the shift in Bragg wavelength is based on the different values of the effective refractive index ( $n_{eff}$ ) of the FBG sensor. The plot shows that the effective refractive index with the smallest value results in higher sensitivity. Furthermore, the FBG with  $n_{eff2}$  achieved a 1.49% increment in sensitivity against that of  $n_{eff3}$  when  $v$  is 0.3.

**Table 2:** FBG Sensitivity at Different Effective Refractive Index at  $v$  of 0.3

Strain ( $\mu\epsilon$ )	$n_{eff1}$ (pm)	$n_{eff2}$ (pm)	$n_{eff3}$ (pm)	$n_{eff4}$ (pm)
0	0	0	0	0
50	71.978	66.050	65.076	55.413
100	143.96	132.10	130.15	110.83
150	215.93	198.15	195.23	166.24
200	287.91	264.20	260.30	221.65
250	359.89	330.25	325.38	277.06

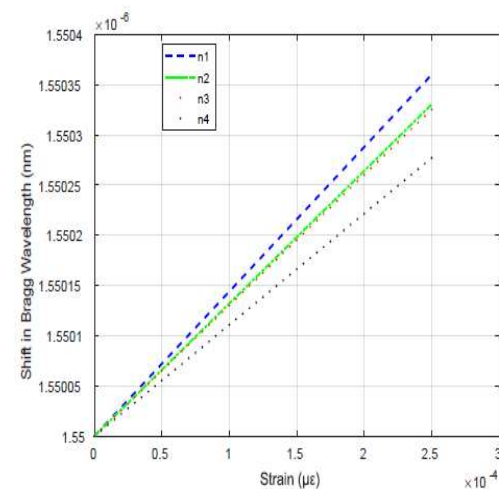


**Figure 4:** Shift in Bragg Wavelength Against Induced Strain on the Composite Structure at Different  $n_{eff}$  when  $v$  is 0.3

In Figure 5, the shifts in Bragg wavelength was plotted against the induced strain on the composite structure at different effective refractive index values ( $n_{eff1} = 1$ ,  $n_{eff2} = 1.44$ ,  $n_{eff3} = 1.5$  and  $n_{eff4} = 2$ ) when  $\nu$  is 0.19525. The plot was obtained from the simulation values in Table 2. Table 2 was generated using equations (2) and (3). From the plot, it is observed that the shift in Bragg wavelength is due to the different values of the effective refractive index ( $n_{eff}$ ) of the FBG sensor. From the plot, it is observed that the shift in Bragg wavelength is based on the different values of the effective refractive index ( $n_{eff}$ ) of the FBG sensor. The plot, it shows that the effective refractive index with the smallest value results in higher sensitivity. Also, the FBG sensor with  $n_{eff2}$  achieved 2.0% increment insensitivity against that of  $n_{eff3}$  when  $\nu$  is 0.19525.

**Table 2:** FBG Sensitivity at Different Effective Refractive Index when  $\nu$  is 0.19525

Strain ( $\mu\epsilon$ )	$n_{eff1}$ (pm)	$n_{eff2}$ (pm)	$n_{eff3}$ (pm)	$n_{eff4}$ (pm)
0	0	0	0	0
50	70.500	62.985	61.750	49.500
100	141.00	125.97	123.50	99.001
150	211.50	188.96	185.25	148.50
200	282.00	251.94	247.00	198.00
250	352.50	314.93	308.75	247.50

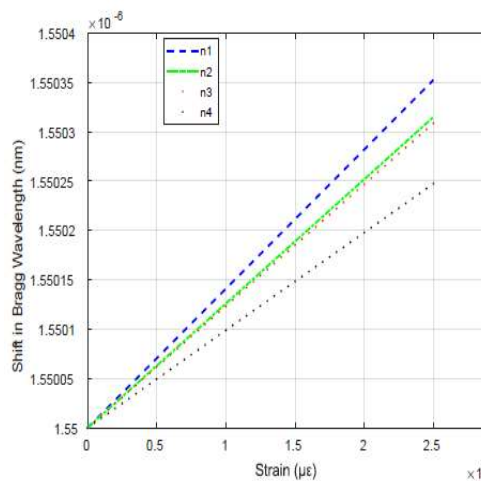


**Figure 5:** Shift in Bragg Wavelength Against Induced Strain on the Composite Structure at Different  $n_{eff}$  when  $\nu$  is 0.19525

## CONCLUSION

In this research, the impact of effective refractive index ( $n_{eff}$ ) on FBG sensor sensitivity was presented. The FBG model with the lowest  $n_{eff}$ , increases the sensor's sensitivity. While the result of the FBG with  $n_{eff2}$  was compared with that of  $n_{eff3}$  and an improvement of 1.49% was obtained at Poisson's ratio ( $\nu$ ) of 0.3 and 2.0% increment in sensitivity at Poisson's ratio ( $\nu$ ) of 0.19525. The increment in the sensor's sensitivity enabled the FBG sensor to be suitable for monitoring structures in harsh environment.

## REFERENCES

- [1] Alcaide, A., Barrera, E., Ruiz, M., & Aranguren, G. (2014). Damage detection on Aerospace structures using PAMELA SHM System. *Instrumentation and Applied Acoustic Research Group*. Retrieved from [https://www.ndt.net/events/aeroNDT2014/a/content/Paper/15\\_Alcaide.pdf](https://www.ndt.net/events/aeroNDT2014/a/content/Paper/15_Alcaide.pdf)
- [2] Amafabia, D. M., Montalvao D., David W. O., & Haritos, G. (2018). A Review of Structural Health Monitoring Techniques as Applied to Composite Structures. *SDHM Structural Durability and Health Monitoring*, 11 (2), 91-147.
- [3] Balogun, T. B. (2018). Integrating bridge maintenance life cycle assessments into bridge design for improved sustainable decision making. The University of the West of England. Retrieved from <http://eprints.uwe.ac.uk/33148/>
- [4] Chen, Q. & Ping, L. (2008). Fibre Bragg Grating and their Applications as Temperature and Humidity Sensors. *Atomic, Molecular and Optical Physics*. ISBN: 978-1-60456-907-0, pp. 235-260
- [5] Dengjiang, W., Jingjing, H., Banglin, D., Xiaopeng, L., & Weifang, Z. (2016). Novel Damage Detection Techniques for Structural Health Monitoring Using a Hybrid Sensor. *Hindawi Publishing Corporation Mathematical Problems in Engineering* Volume 2016, Article ID 3734258, 13.
- [6] Dragic, P.D., Cavillon, M., Ballato, A. & Ballato, J. (2017). A unified materials approach to mitigating optical nonlinearities in optical fibre. II. B. The optical fibre, material additivity and the nonlinear coefficients, *International Journal of Applied Glass Science*, 307–318; DOI: 10.1111/ijag.12329.



- [7] Ganziy, D., Jespersen O., Rose, B., & Bang, O. (2014). An efficient and fast detection algorithm for multimode FBG sensing. *24<sup>th</sup> International Society for Optical Engineering*, Proceedings of SPIE (Vol. 9634), [963445-1].  
Doi:10.1117/12.2194305.
- [8] Garcia, I., Zubia, J., Durana, G., Aldabaldetrek, G. A., María A I., & Joel V. (2015) Optical Fibre Sensors for Aircraft Structural Health Monitoring. *Sensors* 2015, 15, 15494-15519;  
doi:10.3390/s150715494.
- [9] Harpreet, K.B. (2011). Optical Fibre Refractive Index, Voltage and Strain Sensors: Fabrication and Applications; *Centre for Telecommunication and Microelectronics*. Retrieved from <https://core.ac.uk/download/pdf/10836086.pdf>
- [10] Lamberti, A., Luyckx, G., Paepegem, W.V., Rezyat, A., & Vanlanduit, S. (2017). Detection, Localization and Quantification of Impact Events on a Stiffened Composite Panel with Embedded Fibre Bragg Grating Sensor Networks. *Sensors* 2017, 17, 743;  
doi:10.3390/s17040743.
- [11] Lawson, N.J., Correia, R., James, S.W., Partridge, M., Staines, S.E., Gautrey, J.E., Garry, K.P., Holt, J.C., & Tatam, R.P. (2016). Development and application of optical fibre strain and pressure sensors for in-flight measurements. *Measurement Science and Technology Meas. Sci. Technol.* 27 (2016) 104001 (17pp)  
doi:10.1088/0957-233/27/10/104001.
- [12] Matthew, J. N., Rani, W. S., & Lance, W., R. (2016). Large Scale Applications Using FBG Sensors: Determination of In-Flight Loads and Shape of a Composite Aircraft Wing. *NASA Engineering and Safety Centre*. 18;  
doi:10.3390/aerospace3030018.
- [13] Michelle, D., S. (2014). Damage Detection in Composite Materials using PZT Actuators and Sensors for Structural Health Monitoring Department of Electrical and Computer Engineering in the Graduate School of the University of Alabama. Retrieved from <http://acumen.lib.ua.edu/content/u0015/>
- [14] Mishra, P., Charan, K.B., & Sethi, H.K. (2017). Development of FBG Opti-wave system soft wear for structural health monitoring; *International Journal of Engineering Science invention*: 157-163.
- [15] Montalvão, D., Ribeiro A.M.R., & Duarte-Silva, J.A.B. (2011). Experimental Assessment of a Modal-Based Multi-Parameter Method for Locating Damage in Composite Laminates. *Experimental Mechanics* (2011) 51:1473–1488 DOI 0.1007/s11340-011-9472-5.
- [16] Rizwana S., Asim S., Farhan Q., Romana S., Mudassar A., (2018). Effective Refractive Index and V-Parameter Characterization for Guided Modes in Multimode, Nano and Three Layer Optical Fibres. *International Journal of Information Technology and Electrical Engineering ITEE*, volume 7 (3), 20-27.
- [17] Shengbo, S., Jinhao Q., Chao Z., Hongli, J & Li, C., (2016). Multi-damage localization on large complex structures through an extended delay-and-sum based method Structural Health Monitoring, 15(1) 50–64, DOI: 10.1177/1475921715623358.
- [18] Tadamichi, M., & Nelson, D. (2008). A multi-parameter Bragg grating fibre optic sensor and tri-axial strain measurement; *SMART MATERIALS AND STRUCTURES*, 035033 (19pp); doi:10.1088/0964-1726/17/3/035033.
- [19] Voisin, V., Caucheteur C., Mégret, P., & Albert, J. (2014). Anomalous effective strain-optic constants of non-paraxial optical fiber modes, *OPTICS LETTERS* / Vol. 39, No. 3; doi/10.1364/OL.39.000578.
- [20] Zhen, M., & Chen, X. (2018). Fibre Bragg Gratings Sensors for Aircraft Wing Shape Measurement: Recent Applications and Technical Analysis Key Laboratory of Micro-Inertial Instrument and Advanced Navigation Technology. *Sensors* 2019, 19, 55 DOI: 10.3390/s19010055.